PRAMANA
— journal of
physics

Vol. 64, No. 4
April 2005
pp. 535–542

Aspects of stochastic resonance in Josephson junction, bimodal maps and coupled map lattice

G AMBIKA[1], KAMALA MENON[1] and K P HARIKRISHNAN[2]
[1]Department of Physics, Maharaja's College, Cochin 682 011, India
[2]Department of Physics, The Cochin College, Cochin 682 002, India
E-mail: ambika@iucaa.ernet.in; kp_hk2002@yahoo.co.in

Abstract. We present the results of extensive numerical studies on stochastic resonance and its characteristic features in three model systems, namely, a model for Josephson tunnel junctions, the bistable cubic map and a coupled map lattice formed by coupling the cubic maps. Some interesting features regarding the mechanism including multisignal amplification and spatial stochastic resonance are shown.

Keywords. Stochastic resonance; Josephson junction; coupled map lattice.

PACS Nos 5.45.-a; 5.40.Ca; 87.10.+e

1. Introduction

The phenomenon of stochastic resonance (SR) is the noise-induced detection of subthreshold signals or noise-induced transmission of information using the dynamics of nonlinear bistable system or threshold system as the supportive set-up. Since its discovery in 1981 [1], it has been detected and analysed in a variety of systems such as electronic circuits, ring laser, electron paramagnetic resonance system, actual nerve cells and neural networks [2–10]. Recently this phenomenon has been studied in chaotic systems, coupled systems and spatially extended systems [11–15]. The mechanism of SR in a bistable system is explained using the mechanical model with double well potential and is characterised by the signal-to-noise ratio (SNR) computed from the power spectrum of the output. Its bell-shaped variation with the noise amplitude helps to define maximum SNR or peak SNR for an optimum amplitude of input noise. Although SR is most often realised by tuning the input noise amplitude for a given subthreshold signal, environmental noise itself is utilised in real systems or biological systems. Then adapting and designing the system also has a role to play in improving SR in such cases. For threshold-based systems, having one or two stable states, SR depends on the escape mechanism followed by an external reset procedure. Here the difference between the successive escape times gives the inter spike interval (ISI) whose probability shows peaks synchronised with the period of the signal at an optimum noise amplitude.

Here, we analyse the onset and characterisation of SR in three different model systems, namely, a model for Josephson junction (JJ), the bistable cubic map and a coupled map lattice (CML) with the cubic map as the on-site dynamics. We show that JJ combines the features of both bistable and threshold systems and the two mechanisms of SR can be distinguished by using multisignal inputs. It should be mentioned that SR in JJ has been studied in various contexts, such as, in the over-damped limit with multiplicative noise [16] and in a superconducting loop with JJ [17]. But here we consider JJ as a dynamical system with a small damping and in this limit it is almost similar to a pendulum system, having the oscillating and rotatory modes.

The paper is organised as follows: In §2, we present the phenomenon of SR in JJ using a model system. Section 3 includes SR studies on bimodal cubic map and CML. Conclusions are given in §4.

2. Stochastic resonance in a model for Josephson junction

The model system representing the dynamics of a JJ can be written as [16]

$$\begin{aligned} \dot{X} &= Y, \\ \dot{Y} &= -k|Y|Y - \sin X + A\sin Z, \\ \dot{Z} &= \omega_1, \end{aligned} \tag{1}$$

where X is the difference in phase between the electron pair wave functions on both sides of the junction and (k, A, w_1) form the control parameter space with damping k, amplitude of driving A and frequency of driving w_1. The quadratic nature of the damping arises from the inverse dependence of the junction resistance on voltage. One of us (GA) has done extensive numerical analysis of this system [18], wherein regions of bistability in two different oscillating states $S1$ and $S2$ are isolated. These are chosen as the required system parameters for SR studies. Thus, for $k = 0.1$, with $0.2 < A < 0.4$ and $0.5 < w_1 < 0.8$, $S1$ and $S2$ have two well-separated basins of attraction which can be identified by defining a proper distance function D from the origin for $S1$ and $S2$. This helps to detect the shuttling from $S1$ to $S2$ during SR. The time series of D is subjected to spectral analysis after a two-level filtering to calculate the SNR as $10\log(S/N)$ where S is the power of the signal peak and N the average noise level around the peak.

When Gaussian white noise of variance $\sigma = 0.2$ is added and amplitude E tuned properly, the typical variation of SNR is observed at the driving frequency $f_1 = \omega_1/2\pi$, confirming the occurrence of SR in the system (figure 1). When an additional signal of frequency f_2 is added, SR can be observed for both f_1 and f_2 [19]. The calculations are repeated for a range of values f_2 and it is found that for all combinations of (f_1, f_2), only the basic frequencies are amplified and none of the mixed modes are present in the output.

Next, the same system is analysed taking the region of the parameter space where its dynamics resembles a threshold system, i.e., the basin of $S2$ has a large range of initial conditions with escape scenario. The system is reinjected back to its basin by resetting immediately after each escape. This is repeated for a large number

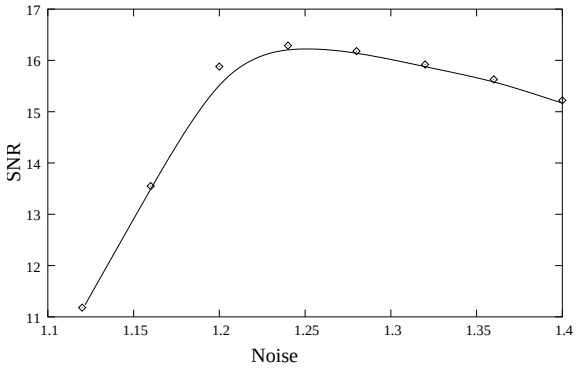

Figure 1. Variation of SNR (in dB) with noise for the system (1) in a bistable set-up with frequency, $f_1 = 0.095$. Here $K = 0.1$, $A = 0.3$.

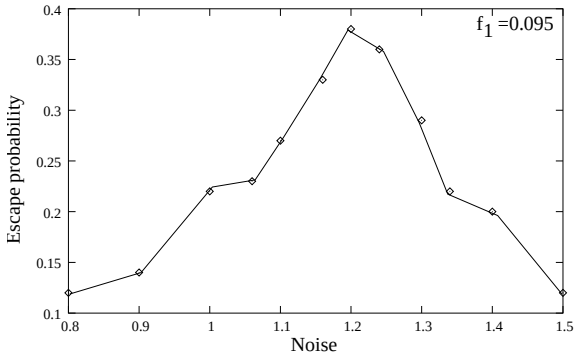

Figure 2. The probability of escape synchronised with the signal for the system (1) in threshold set-up with frequency $f_1 = 0.095$ as a function of noise amplitude.

of escapes and the probability of the ISI, synchronised with the driving signal is calculated. It is found that this probability is maximum at an optimum noise amplitude (figure 2). When this is repeated with the addition of a subthreshold signal of frequency f_2 in the range 0.05 to 0.3, it is found that apart from the two basic frequencies f_1 and f_2, the difference frequency $(f_1 - f_2)/2$ also has a peak, which is in contrast with the bistable mechanism (figure 3). It shows that the two mechanisms of SR are different at least with respect to multisignal inputs. More details regarding SR in the system can be found elsewhere [19].

3. Stochastic resonance in bimodal cubic map and coupled map lattice

Here we consider a typical 2-parameter bimodal cubic map defined by

$$X_{n+1} = b + aX_n - X_n^3. \tag{2}$$

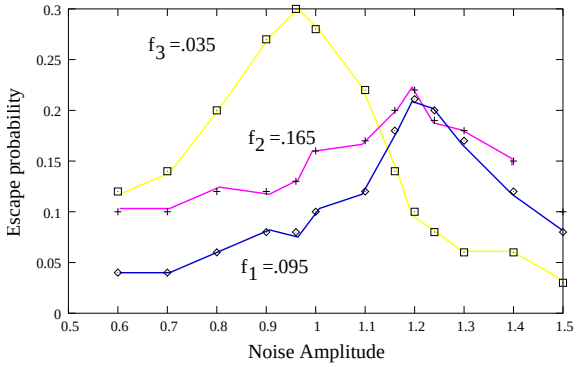

Figure 3. Same as figure 2 when a second frequency $f_2 = 0.165$ is added. Note that apart from f_1 (lowest profile) and f_2, a third frequency $(f_1 - f_2)/2$ is also enhanced.

It has been shown to exhibit a rich variety of dynamical behaviour [20], in particular, a bistable window for b for chosen values of a. When $a = 1.4$, the bistability is in the period-1 state and by varying a, it can be shifted to higher period doubled states and finally to chaotic states for $a = 2.4$. Studies related to SR and resonance due to shuttling with chaotic input of a logistic map (called chaotic resonance) have been reported earlier by the same authors [21]. When two such maps are coupled with linear differential coupling in both ways, the performance of SR is found to improve due to the cooperative behaviour between individual systems. Here, there is an additional design parameter, viz., the coupling strength ε, at an optimum value of which the SNR becomes maximum. Similar results are observed with chaotic input from the logistic map instead of noise [21]. But it is found that Gaussian random noise is more effective in amplifying the signal compared to chaos. This may be because, a chaotic time series is characterised by a power-law behaviour with the power varying on $1/f^{\alpha}$. On the other hand, the Gaussian white noise has a flat power spectrum ($\alpha = 0$) so that power remains constant on all time-scales. The effectiveness of coloured noise in amplifying the signal is currently under study and will be presented elsewhere. When multisignal inputs are used, only the individual frequencies are amplified and none of the mixed modes are found in the output. A typical power spectrum with three input frequencies is shown in figure 4. More details can be found in [22].

We now construct a CML with the bimodal cubic map as the on-site dynamics $f(x_i)$:

$$X^i_{t+1} = (1-\varepsilon) f(x^i_t) + \frac{\varepsilon}{2}\left[f(x^{i-1}_t) + f(x^{i+1}_t)\right], \tag{3}$$

where i denotes the spatial index, t denotes the temporal index and ε the coupling strength. With open boundary conditions $x_t(0) = x_t(n+1) = 0$, with n as the lattice size, we analyse the temporal iterates of the central site with $\varepsilon = 0.01$ and random initial conditions in the range $[-1, 1]$ for all sites. It is found that the iterates remain confined to one of the basins depending on the initial conditions. Next the system is driven independently by a small periodic signal $Z\sin(2\pi pt)$ and

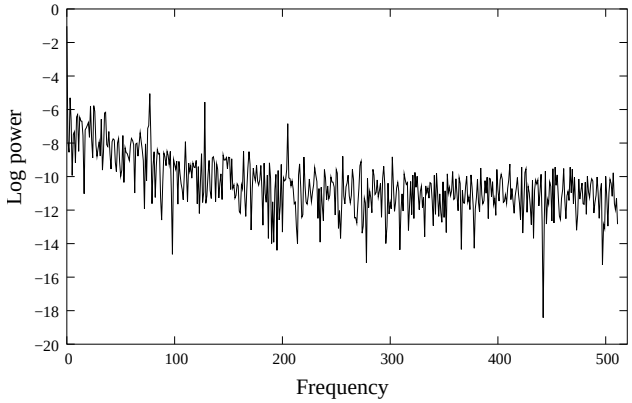

Figure 4. The power spectrum for the composite signal with three basic frequencies, $f_1 = 0.125$, $f_2 = 0.05$ and $f_3 = 0.2$ for two coupled maps using (2). The three peaks due to SR at these three frequencies can be clearly seen.

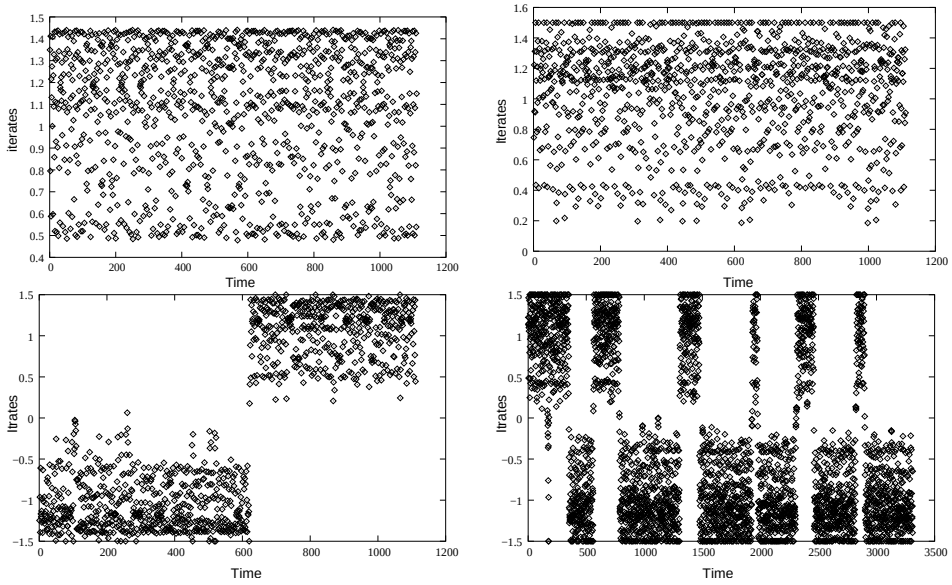

Figure 5. For the CML (3) with $n = 15$ and $\varepsilon = 0.01$, the temporal behaviour of the middle site ($i = 8$) are shown under four different situations. With no signal and noise (top left), with signal alone (top right), with noise alone (bottom left) and with noise and signal together (bottom right).

a Gaussian random noise $E\eta(t)$ and also by a combination of both. Here Z and E represent the amplitude of the signal and noise respectively. The results are shown in figure 5 for a lattice of size $n = 15$. it is clear that there is a systematic shuttling between the basins only when both the signal and noise are present. Similar results are obtained for other n values also.

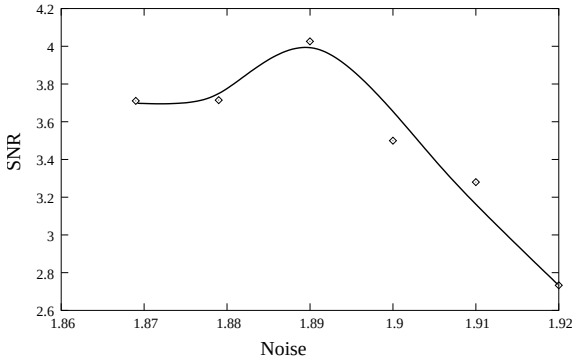

Figure 6. Variation of SNR with noise amplitude for the CML in (3) with $\varepsilon = 0.01$.

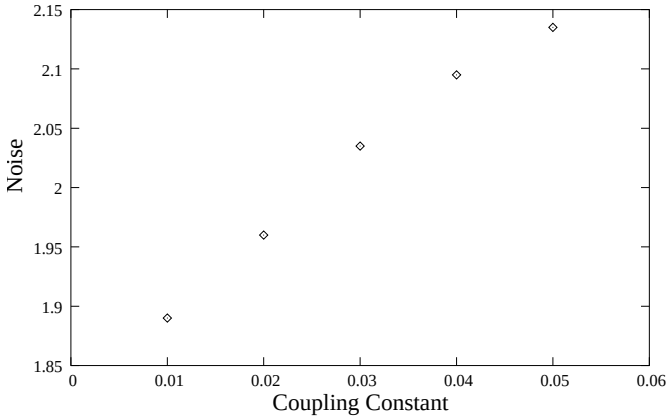

Figure 7. Variation of optimum noise amplitude giving best SNR with the coupling constant ε for the CML.

To pursue SR in the system further, the amplitude and frequency of the signal are fixed at $Z = 0.2$ and $p = 1/8$. With $n = 15$ and $\varepsilon = 0.01$, 512 iterates after a few thousand iterations are chosen to compute the power spectrum with a two-level filtering. The SNR curve shown in figure 6 is then plotted by varying the noise amplitude.

Next, ε is varied from 0.01 to 0.05 and the variation of peak SNR with ε is studied. The variation is not as pronounced as in the case of the linearly coupled cubic maps, the reason being the difference in the nature of coupling. The noise amplitude for maximum SNR is found to vary linearly with ε (figure 7), for the parameter values chosen here.

Another interesting result is the spatial SR shown by the system. To study this, a frozen pattern after a few thousand iterations is used with a lattice size of 512. Now, the signal is static in time and varies along the lattice as $Z\sin(2\pi\text{pi})$ with $Z = 0.05$ and $p = 1/8$. A two-state filtering is done for the output and periodic boundary conditions are used. The behaviour of the lattice for the spatial signal

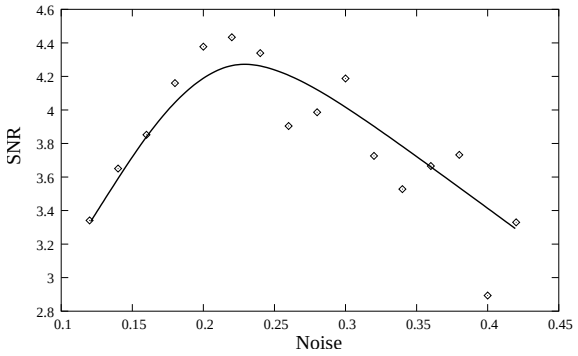

Figure 8. Variation of SNR with noise amplitude for a frozen pattern of the lattice with $n = 512$ with a spatial signal. The average behaviour of a number of frozen patterns after a sufficiently large number of iterations is considered for the calculation. The dots represent numerical data and the continuous line is the best fit.

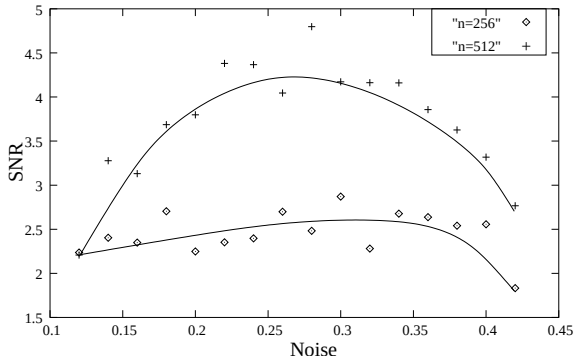

Figure 9. Variation of SNR with noise amplitude for a fixed value of $\varepsilon = 0.001$ but two different values of lattice size.

is similar to the behaviour with temporal signal. The only difference is that, when noise and signal are added, there is a spatial shuttling along the lattice.

The SNR is now calculated taking the spatial series for different values of the noise amplitudes, and is shown in figure 8. It is evident that the lattice points are synchronised with the spatial signal for an optimum noise amplitude, indicating a spatial SR. It should be noted that the idea of a spatial SR has been introduced earlier in a different context in connection with one-dimensional Ising model [23].

Two important parameters of a CML are the lattice size n and the coupling strength ε. In the case of temporal SR, it is found that there is a marked improvement in the SNR values with the increase in n [15]. A similar result is obtained for spatial SR is shown in figure 9, where SNR values are plotted for two different values of n, 256 and 512. But it is found that for a given lattice size, there is no significant change in SNR for the range of ε values considered here.

4. Conclusions

In this paper, three different types of systems are numerically analysed from the viewpoint of SR. Apart from the conventional SR, we study the response of the systems using multisignal inputs also. This enables us to reveal some fundamental difference between the bistable and threshold mechanisms of SR. Another interesting result is that the SR of a signal extended spatially along the lattice. Our results imply that such a signal can be enhanced using an optimum background noise level, which may have potential practical applications.

References

[1] R Benzi, A Sutera and A Vulpiani, *J. Phys.* **A14**, L453 (1981)
[2] E Ippen, J Lindner and W L Ditto, *J. Stat. Phys.* **70**, 437 (1993)
[3] V S Anishchenco, M A Safanova and L O Chua, *Int. J. Bifurcat. Chaos* **4**, 441 (1994)
[4] K Weisenfeld and F Jaramillo, *Chaos* **8**, 539 (1998)
[5] L Gammaitoni, P Hanggi, P Jung and F Marchesoni, *Rec. Mod. Phys.* **70**, 223 (1998)
[6] Mizutani *et al*, *IEICE Trans. Fundamentals* **E82**, 671 (1999)
[7] G Balazsi, L B Kosh and F E Moss, *Chaos* **11**, 563 (2001)
[8] J F Lindner, B K Meadows, T L Marshi, W L Ditto and A L Bulsara, *Int. J. Bifurcat. Chaos* **8**, 767 (1998)
[9] G S Jeon and M Y Choi, *Phys. Rev.* **B66**, 064514 (2002)
[10] A Ganopolski and S Rahmstorf, *Phys. Rev. Lett.* **88**, 038501 (2002)
[11] P M Gade, R Rai and H Singh, *Phys. Rev.* **E66**, 258 (1997)
[12] M Locker, D Cigna, E R Hunt and G A Johnson, *Chaos* **8**, 604 (1998)
[13] A Pikovsky, A Zaikin and M A de la Casa, *Phys. Rev. Lett.* **88**, 050601 (2002)
[14] Hou Zhonghuai, Yang Lingfa, Xiaobin Zuo and Houwen, *Phys. Rev. Lett.* **81**, 2854 (1998)
[15] J F Lindner, B K Meadows, W L Ditto, M E Inchiosa and A R Bulsara, *Phys. Rev. Lett.* **75**, 3 (1995)
[16] V Berdichevsky and M Gitterman, *Phys. Rev.* **E56**, 6340 (1997)
[17] A D Hibbs *et al*, *J. Appl. Phys.* **77**, 2582 (1995)
[18] G Ambika, *Pramana – J. Phys.* **48**, 637 (1997)
[19] K P Harikrishnan and G Ambika, *Phys. Scr.* **71**, 148 (2005)
[20] G Ambika and N V Sujatha, *Pramana – J. Phys.* **54**, 751 (2000)
[21] G Ambika, K P Harikrishnan and N V Sujatha, *Pramana – J. Phys.* **59**, 539 (2002)
[22] K P Harikrishnan and G Ambika, Multisignal amplification by stochastic resonance, *Proc. Natl. Conf. Nonlinear Systems and Dynamics* (IIT Kharagpur, 2003)
[23] Z Neda, A Rusz, E Ravasz, P Lakdawala and P M Gade, *Phys. Rev.* **E60**, R3463 (1999)